

---

# Systematic Evaluation of Causal Discovery in Visual Model Based Reinforcement Learning

---

Nan Rosemary Ke<sup>\*,1,2</sup> Aniket Didolkar<sup>\*,3</sup> Sarthak Mittal<sup>3</sup> Anirudh Goyal<sup>3</sup>  
Guillaume Lajoie<sup>3</sup> Stefan Bauer<sup>6</sup> Danilo Rezende<sup>2</sup>  
Yoshua Bengio<sup>3,†</sup> Michael Mozer<sup>5</sup> Christopher Pal<sup>1,4</sup>

## Abstract

2 Inducing causal relationships from observations is a classic problem in machine  
3 learning. Most work in causality starts from the premise that the causal variables  
4 themselves are observed. However, for AI agents such as robots trying to make  
5 sense of their environment, the only observables are low-level variables like pixels  
6 in images. To generalize well, an agent must induce high-level variables, par-  
7 ticularly those which are causal or are affected by causal variables. A central  
8 goal for AI and causality is thus the joint discovery of abstract representations  
9 and causal structure. However, we note that existing environments for studying  
10 causal induction are poorly suited for this objective because they have complicated  
11 task-specific causal graphs which are impossible to manipulate parametrically (e.g.,  
12 number of nodes, sparsity, causal chain length, etc.). In this work, our goal is to fa-  
13 cilitate research in learning representations of high-level variables as well as causal  
14 structures among them. In order to systematically probe the ability of methods  
15 to identify these variables and structures, we design a suite of benchmarking RL  
16 environments. We evaluate various representation learning algorithms from the  
17 literature and find that explicitly incorporating structure and modularity in models  
18 can help causal induction in model-based reinforcement learning.

## 19 1 Introduction

20 Deep learning methods have made immense progress on many reinforcement learning (RL) tasks  
21 in recent years. However, the performance of these methods still pales in comparison to human  
22 abilities in many cases. Contemporary deep reinforcement learning models have a way to go to  
23 achieve robust generalization [Nichol et al., 2018], efficient planning over flexible timescales [Silver  
24 and Ciosek, 2012], and long-term credit assignment [Osband et al., 2019]. Model-based methods in  
25 RL (MBRL) can potentially mitigate this issue [Schrittwieser et al., 2019]. These methods observe  
26 sequences of state-action pairs, and from these observations are able to learn a self-supervised  
27 model of the environment. With a well-trained world model, these algorithms can then simulate the  
28 environment and look ahead to future events to establish better value estimates, without requiring  
29 expensive interactions with the environment [Sutton, 1991]. Model-based methods can thus be far  
30 more sample-efficient than their model-free counterparts when multiple objectives are to be achieved  
31 in the same environment. However, for model-based approaches to be successful, the learned models  
32 must capture relevant mechanisms that guide the world, i.e., they must discover the right causal  
33 variables and structure. Indeed, models sensitive to causality have been shown to be robust and

---

<sup>\*</sup> Authors contributed equally, <sup>1</sup> Mila, Polytechnique Montréal, <sup>2</sup> Deepmind, <sup>3</sup> Mila, Polytechnique Montréal,  
<sup>4</sup> Element AI, <sup>5</sup> Google AI, <sup>6</sup>Max Planck Institute for Intelligent Systems, <sup>†</sup> CIFAR Senior Fellow Corresponding  
authors: rosemary.nan.ke@gmail.com

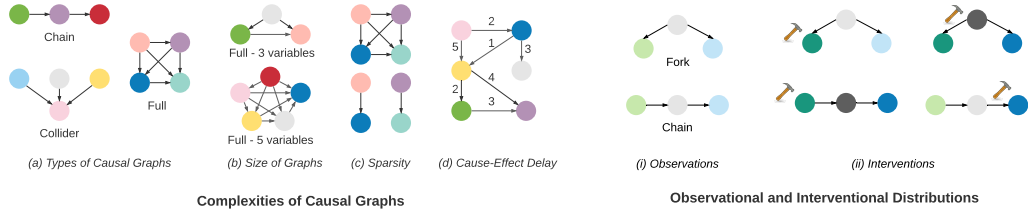


Figure 1: (a)-(d): Different aspects contributing to the complexity of causal graphs. (i), (ii): Difference between observational and interventional data. In RL setting, actions are interventions in the environment. The hammer denotes an intervention. Intervention on a variable not only affects its direct children, but also all reachable variables. Variables impacted by the intervention have a darker shade.

34 easily transferable [Bengio et al., 2019, Ke et al., 2019]. As a result, there has been a recent surge of  
 35 interest in learning causal models for deep reinforcement learning [de Haan et al., 2019, Dasgupta  
 36 et al., 2019, Nair et al., 2019, Goyal et al., 2019, Rezende et al., 2020, Wang et al., 2021]. Yet, many  
 37 challenges remain, and a systematic framework to modulate environment causality structure and  
 38 evaluate models’ capacity to capture it is currently lacking, which motivates this paper.

39 What limits the use of causal modeling approaches in many AI tasks and realistic RL settings is  
 40 that most of the current causal learning literature presumes abstract domain representations in which  
 41 the cause and effect variables are explicit and given [Pearl, 2009]. Methods are needed to automate  
 42 the inference and identification of such causal variables (i.e. *causal induction*) from low-level state  
 43 representations (like images). Although one solution is manual labeling, it is often impractical and  
 44 in some cases impossible to manually label all the causal variables. In some domains, the causal  
 45 structure may not be known. Further, critical causal variables may change from one task to another,  
 46 or from one environment to another. And in unknown environments, one ideally aims for an RL agent  
 47 that could induce the causal structure of the environment from observations and interventions.

48 In this work, we seek to evaluate various model-based approaches parameterized to exploit structure  
 49 of environments purposfully designed to modulate causal relations. We find that modular network  
 50 architectures appear particularly well suited for causal learning. Our conjecture is that causality can  
 51 provide a useful source of inductive bias to improve the learning of world models.

52 **Shortcomings of current RL development environments, and a path forward.** Most existing RL  
 53 environments are not a good fit for investigating causal induction in MBRL, as they have a single  
 54 fixed causal graph, lack proper evaluation and have entangled aspects of causal learning. For instance,  
 55 many tasks have complicated causal structures as well as unobserved confounders. These issues make  
 56 it difficult to measure progress for causal learning. As we look towards the next great challenges for  
 57 RL and AI, there is a need to better understand the implications of varying different aspects of the  
 58 underlying causal graph for various learning procedures.

59 Hence, to systematically study various aspects of causal induction (i.e., learning the right causal graph  
 60 from pixel data), we propose a new suite of environments as a platform for investigating inductive  
 61 biases, causal representations, and learning algorithms. The goal is to disentangle distinct aspects  
 62 of causal learning by allowing the user to choose and modulate various properties of the ground  
 63 truth causal graph, such as the structure and size of the graph, the sparsity of the graph and whether  
 64 variables are observed or not (see Figure 1 (a)-(d)). We also provide evaluation criteria for measuring  
 65 causal induction in MBRL that we argue help measure progress and facilitate further research in  
 66 these directions. We believe that the availability of standard experiments and a platform that can  
 67 easily be extended to test different aspects of causal modeling will play a significant role in speeding  
 68 up progress in MBRL.

69 **Insights and causally sufficient inductive biases.** Using our platform, we investigate the impact  
 70 of explicit structure and modularity for causal induction in MBRL. We evaluated two typical of  
 71 monolithic models (autoencoders and variational autoencoders) and two typical models with explicit  
 72 structure: graph neural networks (GNNs) and modular models (shown in Figure 5). Graph neural  
 73 networks (GNNs) have a factorized representation of variables and can model undirected relationships  
 74 between variables. Modular models also have a factorized representation of variables, along with  
 75 directed edges between variables which can model directed relationship such as  $A$  causing  $B$ , but not  
 76 the other way around. We investigated the performance of such structured approaches on learning  
 77 from causal graphs with varying complexity, such as the size of the graph, the sparsity of the graph  
 78 and the length of cause-effect chains (Figure 1 (a) - (d)).

79 The proposed environment gives novel insights in a number of settings. Especially, we found that  
 80 even our naive implementation of modular networks can scale significantly better compared to other

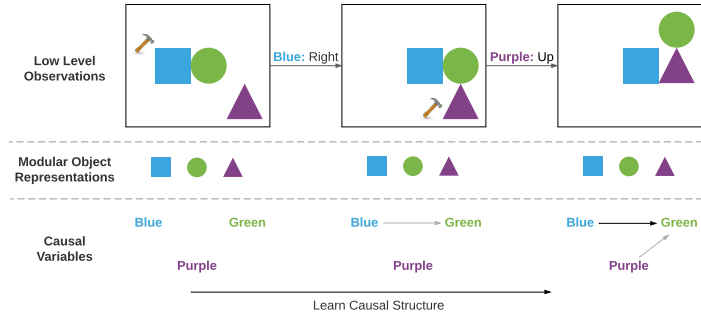


Figure 2: Illustration of the key features of the suite. Environments have objects that interact according to the underlying causal graph which can be based on a subset of objects’ properties. An efficient model should be able to infer the high level causal variables from raw pixel data and learn the underlying causal graph through interactions between these high level causal variables.

81 models (including graph neural networks). This suggests that explicit structure and modularity such  
 82 as factorized representations and directed edges between variables help with causal induction in  
 83 MBRL. We also found that graph neural networks, such as the ones from Kipf et al. [2019] are good  
 84 at modeling pairwise interactions and significantly outperform monolithic models under this setting.  
 85 However, they have difficulty modeling complex causal graphs with long cause-effect chains, such as  
 86 the chain graph (demonstration of chain graphs are found in Figure 1 (i)). Another finding is that  
 87 evaluation metrics such as likelihood and ranking loss do not always correspond to the performance  
 88 of these models in downstream RL tasks.

## 89 2 Environments for causal induction in model-based RL

90 Causal models are frequently described using graphs in which the edges represent causal relationships.  
 91 In these *structural causal models*, the existence of a directed edge from  $A$  to  $B$  indicates that  
 92 intervening on  $A$  directly impacts  $B$ , and the absence of an edge indicates no direct interventional  
 93 impact (see Appendix B for formal definitions).

94 In parallel, world models in MBRL describe the underlying data generating process of the environment  
 95 by modeling the next state given the current state-action pair, where the actions are interventions in  
 96 the environment. Hence, learning world models in MBRL can be seen as a causal induction problem.  
 97 Below, we first outline how a collection of simple causal structures can capture real-world MBRL  
 98 cases, and we propose a set of elemental environments to express them for training. Second, we  
 99 describe precise ways to evaluate models in these environments.

### 100 2.1 Mini-environments: explicit cases for causal modulation in RL

101 The ease with which an agent learns a task greatly depends on the structure of the environment’s  
 102 underlying causal graph. For example, it might be easier to learn causal relationships in a collider  
 103 graph ( see Figure 1(a)) where all interactions are pairwise, meaning that an intervention on one  
 104 variable  $X_i$  impacts no more than one other variable  $X_j$ , hence the cause-effect chain has a length  
 105 of at most 1. However, causal graphs such as full graphs (see Figure 1 (a)) can have more complex  
 106 causal interactions, where intervening on one variable impacts can impact up to  $n - 1$  variables  
 107 for graphs of size  $n$  (see Figure 1). Therefore, one important aspect of understanding a model’s  
 108 performance on causal induction in MBRL is to analyze how well the model performs on causal  
 109 graphs of varying complexity.

110 Important factors that contribute to the complexity of discovering the causal graph are the *structure*,  
 111 *size*, *sparsity of edges* and *length of cause-effect* chains of the causal graph (Figure 1). Presence  
 112 of *unobserved variables* also adds to the complexity. The size of the graph increases complexity  
 113 because the number of possible graphs grows super-exponentially with the *size of the graph* [Eaton  
 114 and Murphy, 2007, Peters et al., 2016, Ke et al., 2019]. The *sparsity of graphs* also impacts the  
 115 difficulty of learning, as observed in [Ke et al., 2019]. Given graphs of the same size, denser graphs  
 116 are often more challenging to learn. Furthermore, the *length of the cause-effect* chains can also impact  
 117 learning. We have observed in our experiments, that graphs with shorter cause-effect lengths such as  
 118 colliders (Figure 1 (a)) can be easier to model as compared to chain graphs with longer cause-effect  
 119 chains. Finally, *unobserved variables* which commonly exist in the real-world can greatly impact  
 120 learning, especially if they are confounding causes (shared causes of observed variables).

121 Taking these factors into account, we designed two suites of (toy) environments: the  
 122 *physics environment* and the *chemistry environment*, which we discuss in more detail in the fol-

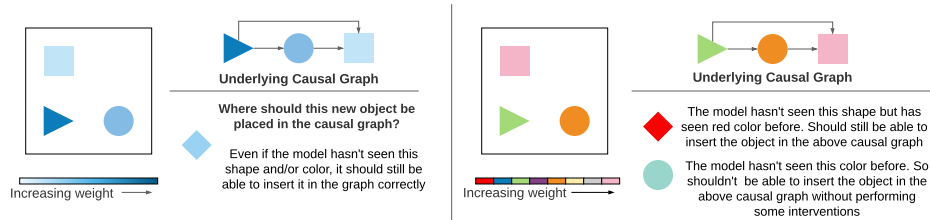


Figure 3: Demonstration of the weighted-block pushing environment (left: observed, right: unobserved) along with the feasible generalizations that the setup provides.

123 lowing section. They are designed with a focus on the underlying causal graph and thus have a  
 124 minimalist design that is easy to visualize.

### 125 2.1.1 Physics environment: Weighted-block pushing

126 The physics environment simulates very simple physics in the world. It consists of blocks of different,  
 127 unique weights. The rule for interaction between blocks is that heavier objects can push lighter ones.  
 128 Interventions amount to move a particular block, and the consequence depends on whether the block  
 129 next to it (if present) is heavier or lighter. For an accurate world model, inferring the weights becomes  
 130 essential. Additionally, one can allow the weight of the objects to be either observed through the  
 131 intensity of the color, or unobserved, leading to two environment settings described below. The  
 132 underlying causal graph is an acyclic tournament, shown in Figure 3.

133 The Physics environment consists of 50 x 50 RGB pixels of renderings of visual scenes in 2D;  
 134 examples are shown in Figures 2-3. Each episode consists of a fixed set of  $k$  objects, drawn without  
 135 replacement; each object is defined by shape. The initial configuration of objects in the scene is  
 136 random. Objects reside on a 5x5 grid of cells; each grid cell is rendered as a 10x10 pixel array, giving  
 137 rise to the 50x50 RGB images. All objects are visible at every time, so the state is Markovian. The  
 138 action space of the agent is a discrete pair  $(x,y)$ , where  $x$  is the index of the object to intervene on  
 139 and  $y$  is a discrete value that sets the value of the intervention. The index-to-object mapping is fixed  
 140 across episodes. The intervention involves pushing the object in a given direction (up, down, left,  
 141 right). The dynamics of that object and others depends on the physics of the domain (e.g., a heavier  
 142 object pushes an adjacent lighter object in the same direction). For more details about the setup,  
 143 please refer to Appendix G.

144 *Fully observed setting.* In the fully observed setting, all objects are given a particular color and the  
 145 weight of each block is represented by the intensity of the color. Once the agent learns this underlying  
 146 causal structure, it does not have to perform interventions on new objects in order to infer they will  
 147 interact with the others.

148 *Unobserved setting.* In this setting, the weight of each object is not directly observable by its color. The  
 149 agent thus needs to interact with the object in order to understand the order of weights associated with  
 150 the blocks. In this case, the weight of objects needs to be inferred through interventions. We consider  
 151 two sub-divisions of this setting - *FixedUnobserved* where there is a fixed assignment between the  
 152 shapes of the objects and their weights and *Unobserved* where there is no fixed assignment between  
 153 the shape and the weight, hence making it a more challenging environment. We refer the reader to  
 154 Appendix G.2 for details.

### 155 2.1.2 Chemistry environment

156 The chemistry environment enables more complexity in the causal structure of the world by allowing  
 157 arbitrary causal graphs. This is depicted by simple chemical reactions, where the state of an element  
 158 can cause changes to another variable's state. The environment consists of a number of objects whose  
 159 positions are kept fixed and thus, uniquely identifiable.

160 The interactions between different objects take place according to the underlying causal graph which  
 161 can either be a randomly generated DAG, or specified by the user. An interaction consists of changing  
 162 the color (state) of a variable. At this point, the color of all variables affected by this variable (accord-  
 163 ing to the causal graph) can change. Interventions change a block's color unconditionally, thus cutting  
 164 the graph edge linking it with its parents in the graph. All transitions are probabilistic and defined by  
 165 conditional probability tables (CPTs). A visualization of the environment can be found in Figure 4.

166 The Chemistry environment (see Figure 4  
 167 for examples) also consists of 50 x 50 RGB  
 168 pixels of renderings of visual scenes in 2D.  
 169 Each episode also consists of a fixed set of  
 170  $k$  objects, drawn without replacement; each  
 171 object is defined by shape. The objects  
 172 does not move within an episode, instead  
 173 the colors of the object can change due to  
 174 an intervention. The action space of the  
 175 agent is still a discrete pair  $(x, y)$ , where  
 176  $x$  is the index of the object to intervene on  
 177 and  $y$  is a discrete value that sets the the  
 178 color that the object is changed to.

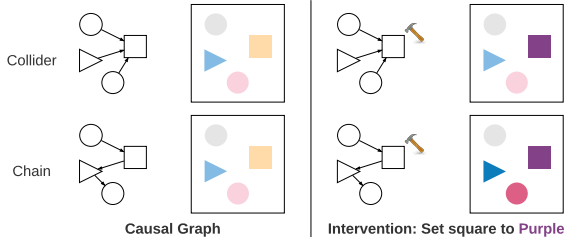


Figure 4: Demonstration of the vanilla chemistry environment (left: ground truth causal graph and a sample from it - same sample shown to demonstrate the affect of interventions, right: the affect of interventions and how far they affect based on underlying causal graph)

179 This environment allows for a complete  
 180 and thorough testing of causal models as  
 181 there are various degrees of complexities which can be easily tuned such as: (1) Complexity of the  
 182 graph: We can test any model on many different graphs thus ensuring that a models performance is  
 183 not only limited to a few select graphs. (2) Stochasticity: By tuning the skewness of the probability  
 184 distribution of each object we can test how good is a given model in modelling data uncertainty. In  
 185 addition to this we can also tune the number of object or the number of colors to test whether the  
 186 model generalizes to larger graphs and more colors. A causally correct model should be able to infer  
 187 the causal relationships between observed objects, as well as their respective color distribution and its  
 188 dependence on a causal parent’s distribution.

## 189 2.2 Evaluating causal models

190 In much of the existing literature, evaluation of learned causal models is based on the structural  
 191 difference between the learned graph and the ground-truth graph [Peters et al., 2016, Zheng et al.,  
 192 2018]. However, this may not be applicable for most deep RL algorithms, as they do not necessarily  
 193 learn an explicit causal structure [Dasgupta et al., 2019, Ke et al., 2020]. Even if a structure is learned,  
 194 it may not be unique as several variable permutations can be equivalent, introducing an additional  
 195 evaluation burden.

196 Another possibility is to exhaustively evaluate models on all possible intervention predictions and  
 197 all environment states, a process that quickly becomes intractable even for small environments. We  
 198 therefore propose a few evaluation methods that can be used as a surrogate metrics to measure the  
 199 model’s performance on recovering the correct causal structure.

200 *Predicting Intervention Outcomes.* While it may not be feasible to predict all intervention outcomes  
 201 in an RL environment, we propose that evaluating predictions on a subset of interventions provides  
 202 an informative evaluation. Here, the test data is collected from the same environment used in training,  
 203 ensuring a single underlying causal graph. Test data is generated from new episodes that are unseen  
 204 during training. All interventions (actions) in the test episodes are randomly sampled and we evaluate  
 205 the model’s performance on this test set.

206 *Zero Shot Transfer.* Here, we test the model’s ability to generalize to unseen test environments, where  
 207 the environment does not have exactly the same causal graph as training, but training and test causal  
 208 graphs share some similarity.

209 For example, in the *observed* Physics environment, a model that has learned the underlying causal  
 210 relationship between color intensity and weight would be able to generalize to new variables with a  
 211 novel color intensity.

212 *Downstream RL Tasks.* Downstream RL tasks that require a good understanding of the underlying  
 213 causal graph of the environment are also good metrics for measuring the model’s performance. For  
 214 example, in the *physics environment*, we can provide the model with a target configuration in the  
 215 form of some specific arrangement of blocks on a grid and the model needs to perform actions in  
 216 the environment to reach the target configuration. Models that capture causal relationships between  
 217 objects should achieve the target configuration more easily (as it is can predict intervention outcomes).  
 218 For more details about this setup, please refer to [Appendix E](#).

219 *Metrics.* We also evaluate the learned models on ranking metrics in the latent space as well as  
 220 reconstruction-based metrics in the observation space [Kipf et al., 2019]. In particular we measure  
 221 and report Hits at Rank 1 (H@1), Mean Reciprocal Rank (MRR) and Reconstruction loss for  
 222 evaluation in standard as well as transfer testing settings. We report these metrics for 1, 5 and 10  
 223 steps of prediction in the latent space (refer Appendix C).

### 224 3 Models

225 A large variety of neural network models have been proposed as world models in MBRL. These  
 226 models can roughly be divided into two categories: *monolithic models* and models that have *structure*  
 227 and *modularity*. *Monolithic models* typically have no explicit structure (other than layers). Some  
 228 typical monolithic models are Autoencoders and Variational Autoencoders [Kingma and Welling,  
 229 2013, Rezende et al., 2014]. Conversely, *structured* models have explicit architecture built into (or  
 230 learned by) the model. Examples of such models are ones based on graph neural networks [Battaglia  
 231 et al., 2016, Van Steenkiste et al., 2018, Kipf et al., 2019, Veerapaneni et al., 2020] and modular  
 232 models [Ke et al., 2020, Goyal et al., 2019, Mittal et al., 2020, Goyal et al., 2020]. We picked some  
 233 commonly used models from these categories and evaluated their performance to understand their  
 234 ability for causal induction in MBRL.

235 To disentangle the architectural biases and effects of different training methodologies,  
 236 we trained all the models on both likelihood based and contrastive losses, respectively. All models share three common  
 237 components: *encoder*, *decoder* and *transition model*. We follow a similar training  
 238 procedure as in Ha and Schmidhuber [2018], Kipf et al. [2019]. Details of the archi-  
 239 tectures as well as the training protocols and losses can be found in Appendix F.

#### 246 3.1 Monolithic Models

247 We evaluate causal induction on two commonly used monolithic models: multilayered autoencoders and variational autoencoders. We follow a similar setup as in Ha and Schmidhuber [2018]. These models do not have strong inductive biases other than the number of layers used.

#### 254 3.2 Modular and Structured Models

255 Several forms of structure can be included in neural networks, including *modularity*, *factorized variables*, and *directed rules*.

257 Taking the three factors into account, we consider two types of structured models in our paper, *graph neural networks* (GNN) and so called *modular networks*. Graph neural networks (GNN) [Gilmer et al., 2017, Tacchetti et al., 2018, Battaglia et al., 2018, Kipf et al., 2019] is a widely adopted relational model that have a factorized representation of variables and models pairwise interactions between objects while being permutation invariant. In particular, we consider the C-SWM model [Kipf et al., 2019], which is a state-of-art GNN used for modeling object interactions. Similar to most GNNs, the C-SWM model learns factorized representations of different objects but for modelling dynamics it considers all possible pairwise interactions, and hence the transition model is monolithic (i.e., not a modular transition model).

266 Modular networks on the other hand are composed of an initial encoder that factorizes inputs (images), and then a *modular transition model* (MTM) -  $M$ . This internal model is tasked to create separate factored representations for each objects in the environment, while taking into account all other objects' representations. This model also learns interactions between objects. The rules learned here are *directed rules*.

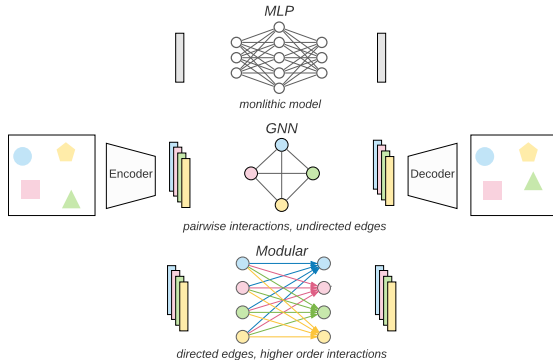


Figure 5: All models have 3 components: *encoder*, *decoder* and *transition model*. The transition models can either be monolithic, modular model or graph neural networks (GNNs). Monolithic models don't have explicit structure. GNNs have factorized representation of variables. Modular models have factorized representation of both variables and directed edges to potentially model causal relationships, e.g.  $A$  causing  $B$ .

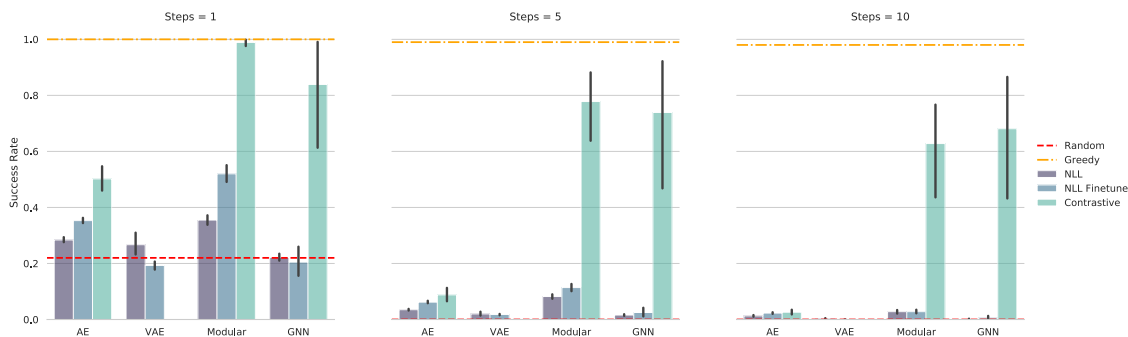


Figure 6: Success Rate (*higher is better*) for different models and training losses for 1, 5 and 10 step prediction for the Fixed Unobserved Physics environment setting with 5 objects. Here, (a) Random stands for a random policy, (b) greedy is the policy with best greedy actions, (c) NLL are models trained in 2 stages: pretraining the encoder/ decoder, following by only training the transition model, (d) NLL with finetune are models in 3 stages: pretraining the encoder/ decoder, following by only training the transition model and then finetuning the encoder, decoder and transition models together. (e) Contrastive are models trained using a contrastive loss. The GNN and Modular models trained on contrastive loss significantly outperform the monolithic models (autoencoders and VAE). The margin significantly increases as the number of steps to reach the goal increase, suggesting that models with explicit structure and modularity have a much better understanding of the world.

## 271 4 Experiments

272 Our experiments seek to answer the following questions: (a) Does explicit structure and modularity  
 273 help for causal induction in MBRL? If so, then what type of structures provide good inductive bias  
 274 for causal induction in MBRL? (b) How do different objective functions (likelihood or contrastive)  
 275 impact learning? (c) How do different models scale to complex causal graphs? (d) Do prediction  
 276 metrics (likelihood and ranking metrics) correspond to better downstream RL performance? (e) What  
 277 are good evaluation criteria for causal induction in MBRL?

278 We report the performance of our models on both the Physics and the Chemistry environments,  
 279 and refer the readers to [Appendix F](#) for implementation details.. All models are trained using the  
 280 procedure described in [Appendix F.2](#) and are evaluated based on *ranking* and *likelihood metrics* on  
 281 1, 5 and 10 step predictions. For the Chemistry environment, we evaluate the models on causal graphs  
 282 with varying complexity, namely - *chain*, *collider* and *full* graphs. These graphs vary in the *sparsity*  
 283 *of edges* and the *length of cause-effect chains*. For the Physics environment, we evaluate the model in  
 284 the fully observed setting as well as the unobserved setting.

### 285 4.1 Data

286 The autoencoder,VAE, modularand GNN models are trained on sequences generated by an agent  
 287 following a random policy. The training data consists of 1,000 sequences consisting of 100 frames  
 288 per sequence. The validation data consists of 1,000 sequences with 100 frames per sequence. The  
 289 test data consists of 10,000 sequences with 10 frames per sequence.

### 290 4.2 Explicit structure and causal induction

291 We found that for both the Physics and the Chemistry environments, models with explicit structure  
 292 outperform monolithic models on both prediction metrics and downstream RL performances. In  
 293 particular, models with explicit structure (GNNs and modular models) scale better to graphs of *larger*  
 294 *size* and *longer cause-effect chains*.

295 The Physics environment has a complex underlying causal graph (full graph: refer [Figure 1](#) (a)). We  
 296 found that GNNs performed well in this environment with 3 variables. They achieved good prediction  
 297 metrics ([Figure 8](#)) and high RL performance ([Figure 14](#)) even at longer timescales. However, their  
 298 performance drops significantly on environments with 5 objects both in terms of prediction metrics  
 299 ([Figure 9](#)) and RL performance ([Figure 15](#)). We also see in [Figures 9](#) and [15](#) that modular models  
 300 scale much better compared to all other models, suggesting that they hold an advantage for *larger*  
 301 *causal graphs*. Further, modular models and GNNs when evaluated on zero shot settings outperform  
 302 monolithic models by a significant margin ([Figures 20](#) and [21](#) and [Tables 15](#) and [16](#)).

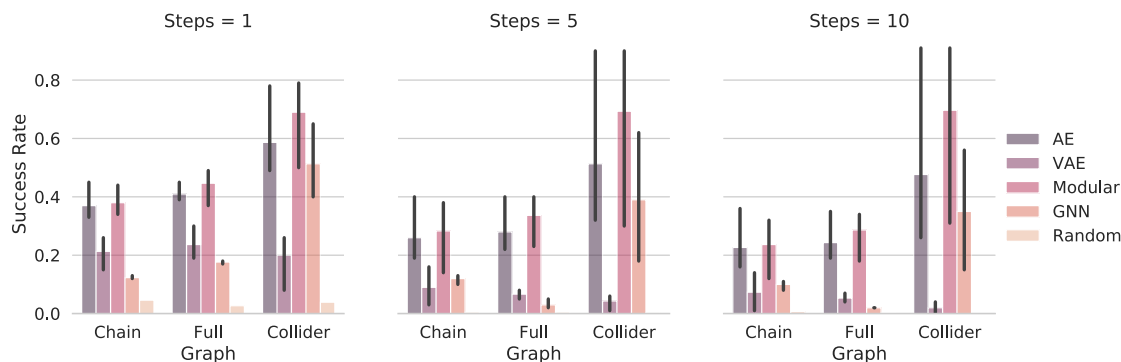


Figure 7: Success rate (higher is better) for different models evaluated on 1, 5 and 10 step predictions for the static chemistry environment with 5 objects and 5 colors. The results are grouped in types of causal graphs for the environment, refer to section 1(a) for illustrations of different types of causal graphs. Chain and full graphs are significantly more challenging compared to collider graphs. This suggests that causal relationships in chain and full graphs with longer cause and effect chains are more challenging to learn compared to the collider graphs, which has only pairwise interactions. Modular models outperform all other models in almost all cases, this is an indication that introducing structure in the form of modularity is an important inductive bias for learning causal models.

303 For the chemistry environment, we find that modular models outperform all other models for almost  
 304 all causal graphs in terms of both prediction metrics (Figure 24) and RL performance (Figures 7  
 305 and 26). This is especially true on more complex causal graphs, such as *chain* and *full* graphs which  
 306 have long cause-effect chains. This suggests that modular models scales better to more complex  
 307 causal graphs.

308 Overall, these results suggest that structure, and in particular modularity, help causal induction in  
 309 MBRL when scaling up to larger and more complex causal graphs. The performance comparisons  
 310 on modular networks and C-SWM [Kipf et al., 2019] suggest that both factorized representation of  
 311 variables and directed edges between variables can help for causal induction in MBRL.

### 312 4.3 Complexity of the Underlying Causal Graph

313 There are several ways to vary complexity in a causal graph: *size of the graph*, *sparsity of edges*  
 314 and *length of cause-effect chain* (Figure 1). Increasing the size of the graph significantly impacts all  
 315 models’ performances. We evaluate models on the Physics environments with 3 objects (Figure 8)  
 316 and 5 objects (Figure 9) and find that increasing the number of objects from 3 to 5 has a significant  
 317 impact on performance. Modular models achieve over 90 on ranking metrics over 10-step prediction  
 318 for 3 objects while for 5 objects, they achieve only 50 (almost half the performance on 3 objects).  
 319 A similar pattern is found in almost all models. Another factor impacting complexity of the graph  
 320 is the *length of cause-effect chain*. We see that collider graphs are the easiest to learn, with modular  
 321 models and autoencoders significantly outperforming all other models (Figure 24). This is because the  
 322 collider graph has short pair-wise interactions, i.e, intervention on any node in a collider graph can  
 323 impact at most one other node. Chain and full graphs are significantly more challenging because of  
 324 longer cause-effect chains. For a chain or a full graph of  $n$  nodes, an intervention on the  $k^{th}$  node can  
 325 impact all the subsequent  $(n - k)$  nodes. Modeling interventions on chain and full graphs require  
 326 modeling more than pairwise relationships, hence, making it much more challenging. We find that  
 327 modular models slightly outperform all other models on these graphs.

### 328 4.4 Prediction Metrics and RL Performance

329 As discussed in Section 2.2, there are multiple evaluation metrics based on either prediction metrics or  
 330 RL performance. The performance of the model on one metric may not necessarily transfer to another.  
 331 We would like to analyze if this is the case for the models trained under various environments. We first  
 332 note that while the ranking metrics were relatively good for most models on physics environments,  
 333 most of them only did slightly better than a random policy on downstream RL, especially on larger  
 334 graphs (Figures Figure 8 - 13 and Table 3 - 8 for ranking metrics; Figure 14 - 19 and Table 9 - 14 for  
 335 downstream RL). Figures 22, 23 and 28 show scatter plots for each pair of losses, with one loss on  
 336 each axis. While there is some correlation between ranking metric and RL performance (Modular  
 337 and GNN; Figure 22), we did not find this trend to be consistent across models and environment  
 338 settings. We feel that these results give further evidence of need to evaluate on RL performance.



## 339 4.5 Training objectives and learning

340 Likelihood loss and contrastive loss [Oord et al., 2018, Kipf et al., 2019] are two frequently used  
341 objectives for training world models in MBRL. We trained the models under each of these objective  
342 functions to understand how they impact learning. In almost all cases, models with explicit structure  
343 (modular models and GNNs) trained on contrastive loss perform better in terms of ranking loss  
344 compared to those trained on likelihood loss (refer to Figure 8 - 13). We don't see a very clear  
345 trend between training objective and downstream RL performance but we do see a few cases where  
346 contrastively trained models performed much better than others (refer to Figures 6, 14, 18 and 19 and  
347 Tables 9, 13 and 14). For other key insights and experimental conclusions on different environments,  
348 we refer the readers to Appendix G.6 for the physics environment and Appendix H.3 for the chemistry  
349 environment.

## 350 5 Related work

351 *Video Prediction and Visual Question Answering.* There exist a number of video prediction [Yi et al.,  
352 2019, Baradel et al., 2019] and visual question answering [Johnson et al., 2017] datasets that also  
353 make use of a blocks world for visual representation. Though these datasets can appear visually  
354 similar to ours at first glance, they lack two essential ingredients for systematically evaluating models  
355 for causal induction in MBRL. The first is that they do not allow active interventions and hence make  
356 it challenging for evaluating model-based reinforcement learning algorithms. Another key point is  
357 that these environments do not allow one to systematically perturb different aspects of causal graphs,  
358 hence, preventing to systematically study the performances of models for causal induction.

359 *RL Environments.* There exist several benchmarks for multi-task learning for robotics (Meta-World  
360 [Yu et al., 2019] and RL Bench [James et al., 2020]), for Physical reasoning Bakhtin et al. [2019]  
361 and for video gaming domain (Arcade Learning Environment, CoinRun [Cobbe et al., 2018], Sonic  
362 Benchmark [Machado et al., 2018], MazeBase [Nichol et al., 2018] and BabyAI [Chevalier-Boisvert  
363 et al., 2018]). However, as mentioned earlier, these benchmarks do not allow one to systematically  
364 control different aspects of causal models (such as the structure, the sparsity of edges and the size of  
365 the graph), hence making it difficult to systematically study causal induction in MBRL. The Alchemy  
366 [Wang et al., 2021] environment, which was released earlier this year, moves a step towards causal  
367 induction for meta-RL. Though the environment allows for some level of control of the underlying  
368 causal structures of the environment, it still does so in a limited way.

369 *Block World.* The AI community has been using the "blocks world" for decades as a testbed for  
370 various AI problems, including learning theory [Winston, 1970], natural language [Winograd, 1972],  
371 and planning [Fahlman, 1974]. Block world allows to easily vary different aspects of the underlying  
372 causal structure, and also allow interventions to be performed on many high level variables of the  
373 environment giving rise to a large space of tasks which have well-defined relations between them.

## 374 6 Discussions and conclusions

375 In our work, we focus on studying various model-based approaches for causal induction in model-  
376 based RL. We highlighted the limitations of existing benchmarks and introduced a novel suite of  
377 environments that can help measure progress and facilitate research in this direction. We evaluated  
378 various models under many different settings and discuss the essential problems and challenges in  
379 combining both fields i.e ingredients, that we believe are common in the real world, such as modular  
380 factorization of the objects and interactions of objects governed by some unknown rules. Using a  
381 proposed evaluation framework, we demonstrate that structural inductive biases are beneficial to  
382 learning causal relationships and yield significantly improved performances in learning world models.

383 **Limitations and Future Work.** There are some limitations of this work that can be explored in  
384 interesting directions in the future. One direction is extending the environments to settings such as  
385 meta-learning, where different causal graphs are set for each episode of training. Another limitation of  
386 our work is that in the environments which we propose the effect occurs immediately after the cause,  
387 but in real world settings the effect may sometimes be delayed. For example, if a person smokes, it  
388 can take variable amount of time until they get cancer. This is very relevant for reinforcement learning,  
389 as this is tightly related to credit assignment in RL. Future works could explore environments where  
390 the relation between cause and effect does not occur at fixed time-scales.

391 **Social Impact.** The authors do not foresee negative social impact of this work beyond that which  
392 could arise from general improvements in ML.

## 393 References

- 394 Anton Bakhtin, Laurens van der Maaten, Justin Johnson, Laura Gustafson, and Ross Girshick. Phyre:  
395 A new benchmark for physical reasoning. In *Advances in Neural Information Processing Systems*,  
396 pages 5082–5093, 2019.
- 397 Fabien Baradel, Natalia Neverova, Julien Mille, Greg Mori, and Christian Wolf. Cophy: Counterfac-  
398 tual learning of physical dynamics. *arXiv preprint arXiv:1909.12000*, 2019.
- 399 Peter Battaglia, Razvan Pascanu, Matthew Lai, Danilo Jimenez Rezende, et al. Interaction networks  
400 for learning about objects, relations and physics. In *Advances in neural information processing*  
401 *systems*, pages 4502–4510, 2016.
- 402 Peter W Battaglia, Jessica B Hamrick, Victor Bapst, Alvaro Sanchez-Gonzalez, Vinicius Zambaldi,  
403 Mateusz Malinowski, Andrea Tacchetti, David Raposo, Adam Santoro, Ryan Faulkner, et al.  
404 Relational inductive biases, deep learning, and graph networks. *arXiv preprint arXiv:1806.01261*,  
405 2018.
- 406 Yoshua Bengio, Tristan Deleu, Nasim Rahaman, Rosemary Ke, Sébastien Lachapelle, Olexa Bilaniuk,  
407 Anirudh Goyal, and Christopher Pal. A meta-transfer objective for learning to disentangle causal  
408 mechanisms. *arXiv preprint arXiv:1901.10912*, 2019.
- 409 Maxime Chevalier-Boisvert, Dzmitry Bahdanau, Salem Lahlou, Lucas Willems, Chitwan Saharia,  
410 Thien Huu Nguyen, and Yoshua Bengio. Babyai: First steps towards grounded language learning  
411 with a human in the loop. *arXiv preprint arXiv:1810.08272*, 2018.
- 412 Karl Cobbe, Oleg Klimov, Chris Hesse, Taehoon Kim, and John Schulman. Quantifying generalization  
413 in reinforcement learning. *arXiv preprint arXiv:1812.02341*, 2018.
- 414 Ishita Dasgupta, Jane Wang, Silvia Chiappa, Jovana Mitrovic, Pedro Ortega, David Raposo, Edward  
415 Hughes, Peter Battaglia, Matthew Botvinick, and Zeb Kurth-Nelson. Causal reasoning from  
416 meta-reinforcement learning. *arXiv preprint arXiv:1901.08162*, 2019.
- 417 Pim de Haan, Dinesh Jayaraman, and Sergey Levine. Causal confusion in imitation learning. In  
418 *Advances in Neural Information Processing Systems*, pages 11698–11709, 2019.
- 419 Daniel Eaton and Kevin Murphy. Exact bayesian structure learning from uncertain interventions. In  
420 *Artificial Intelligence and Statistics*, pages 107–114, 2007.
- 421 Scott Elliott Fahlman. A planning system for robot construction tasks. *Artificial intelligence*, 5(1):  
422 1–49, 1974.
- 423 Justin Gilmer, Samuel S Schoenholz, Patrick F Riley, Oriol Vinyals, and George E Dahl. Neural  
424 message passing for quantum chemistry. In *Proceedings of the 34th International Conference on*  
425 *Machine Learning-Volume 70*, pages 1263–1272. JMLR. org, 2017.
- 426 Anirudh Goyal, Alex Lamb, Jordan Hoffmann, Shagun Sodhani, Sergey Levine, Yoshua Bengio, and  
427 Bernhard Schölkopf. Recurrent independent mechanisms. *arXiv preprint arXiv:1909.10893*, 2019.
- 428 Anirudh Goyal, Alex Lamb, Phanideep Gampa, Philippe Beaudoin, Sergey Levine, Charles Blundell,  
429 Yoshua Bengio, and Michael Mozer. Object files and schemata: Factorizing declarative and  
430 procedural knowledge in dynamical systems. *arXiv preprint arXiv:2006.16225*, 2020.
- 431 David Ha and Jürgen Schmidhuber. World models. *arXiv preprint arXiv:1803.10122*, 2018.
- 432 Stephen James, Zicong Ma, David Rovick Arrojo, and Andrew J Davison. Rlbench: The robot  
433 learning benchmark & learning environment. *IEEE Robotics and Automation Letters*, 5(2):3019–  
434 3026, 2020.
- 435 Justin Johnson, Bharath Hariharan, Laurens van der Maaten, Li Fei-Fei, C Lawrence Zitnick, and  
436 Ross Girshick. Clevr: A diagnostic dataset for compositional language and elementary visual  
437 reasoning. In *Proceedings of the IEEE Conference on Computer Vision and Pattern Recognition*,  
438 pages 2901–2910, 2017.

- 439 Nan Rosemary Ke, Olexa Bilaniuk, Anirudh Goyal, Stefan Bauer, Hugo Larochelle, Chris Pal, and  
440 Yoshua Bengio. Learning neural causal models from unknown interventions. *arXiv preprint*  
441 *arXiv:1910.01075*, 2019.
- 442 Nan Rosemary Ke, Jane Wang, Jovana Mitrovic, Martin Szummer, Danilo J Rezende, et al. Amortized  
443 learning of neural causal representations. *arXiv preprint arXiv:2008.09301*, 2020.
- 444 Diederik P Kingma and Jimmy Ba. Adam: A method for stochastic optimization. *arXiv preprint*  
445 *arXiv:1412.6980*, 2014.
- 446 Diederik P Kingma and Max Welling. Auto-encoding variational bayes. *arXiv preprint*  
447 *arXiv:1312.6114*, 2013.
- 448 Thomas Kipf, Elise van der Pol, and Max Welling. Contrastive learning of structured world models.  
449 *arXiv preprint arXiv:1911.12247*, 2019.
- 450 Marlos C Machado, Marc G Bellemare, Erik Talvitie, Joel Veness, Matthew Hausknecht, and Michael  
451 Bowling. Revisiting the arcade learning environment: Evaluation protocols and open problems for  
452 general agents. *Journal of Artificial Intelligence Research*, 61:523–562, 2018.
- 453 Sarthak Mittal, Alex Lamb, Anirudh Goyal, Vikram Voleti, Murray Shanahan, Guillaume Lajoie,  
454 Michael Mozer, and Yoshua Bengio. Learning to combine top-down and bottom-up signals in  
455 recurrent neural networks with attention over modules. *arXiv preprint arXiv:2006.16981*, 2020.
- 456 Suraj Nair, Yuke Zhu, Silvio Savarese, and Li Fei-Fei. Causal induction from visual observations for  
457 goal directed tasks. *arXiv preprint arXiv:1910.01751*, 2019.
- 458 Alex Nichol, Vicki Pfau, Christopher Hesse, Oleg Klimov, and John Schulman. Gotta learn fast: A  
459 new benchmark for generalization in rl. *arXiv preprint arXiv:1804.03720*, 2018.
- 460 Aaron van den Oord, Yazhe Li, and Oriol Vinyals. Representation learning with contrastive predictive  
461 coding. *arXiv preprint arXiv:1807.03748*, 2018.
- 462 Ian Osband, Yotam Doron, Matteo Hessel, John Aslanides, Eren Sezener, Andre Saraiva, Katrina  
463 McKinney, Tor Lattimore, Csaba Szepesvari, Satinder Singh, et al. Behaviour suite for reinforce-  
464 ment learning. *arXiv preprint arXiv:1908.03568*, 2019.
- 465 Judea Pearl. *Causality*. Cambridge university press, 2009.
- 466 Jonas Peters, Peter Bühlmann, and Nicolai Meinshausen. Causal inference by using invariant  
467 prediction: identification and confidence intervals. *Journal of the Royal Statistical Society: Series*  
468 *B (Statistical Methodology)*, 78(5):947–1012, 2016.
- 469 Jonas Peters, Dominik Janzing, and Bernhard Schölkopf. *Elements of causal inference: foundations*  
470 *and learning algorithms*. MIT press, 2017.
- 471 Danilo J Rezende, Ivo Danihelka, George Papamakarios, Nan Rosemary Ke, Ray Jiang, Theophane  
472 Weber, Karol Gregor, Hamza Merzic, Fabio Viola, Jane Wang, et al. Causally correct partial  
473 models for reinforcement learning. *arXiv preprint arXiv:2002.02836*, 2020.
- 474 Danilo Jimenez Rezende, Shakir Mohamed, and Daan Wierstra. Stochastic backpropagation and  
475 approximate inference in deep generative models. In *Proceedings of The 31st International*  
476 *Conference on Machine Learning*, pages 1278–1286, 2014.
- 477 Julian Schrittwieser, Ioannis Antonoglou, Thomas Hubert, Karen Simonyan, Laurent Sifre, Simon  
478 Schmitt, Arthur Guez, Edward Lockhart, Demis Hassabis, Thore Graepel, et al. Mastering atari,  
479 go, chess and shogi by planning with a learned model. *arXiv preprint arXiv:1911.08265*, 2019.
- 480 John Schulman, Filip Wolski, Prafulla Dhariwal, Alec Radford, and Oleg Klimov. Proximal policy  
481 optimization algorithms. *arXiv preprint arXiv:1707.06347*, 2017.
- 482 David Silver and Kamil Ciosek. Compositional planning using optimal option models. *arXiv preprint*  
483 *arXiv:1206.6473*, 2012.

- 484 Richard S Sutton. Dyna, an integrated architecture for learning, planning, and reacting. *ACM Sigart*  
485 *Bulletin*, 2(4):160–163, 1991.
- 486 Andrea Tacchetti, H Francis Song, Pedro AM Mediano, Vinicius Zambaldi, Neil C Rabinowitz, Thore  
487 Graepel, Matthew Botvinick, and Peter W Battaglia. Relational forward models for multi-agent  
488 learning. *arXiv preprint arXiv:1809.11044*, 2018.
- 489 Sjoerd Van Steenkiste, Michael Chang, Klaus Greff, and Jürgen Schmidhuber. Relational neural  
490 expectation maximization: Unsupervised discovery of objects and their interactions. *arXiv preprint*  
491 *arXiv:1802.10353*, 2018.
- 492 Rishi Veerapaneni, John D Co-Reyes, Michael Chang, Michael Janner, Chelsea Finn, Jiajun Wu,  
493 Joshua Tenenbaum, and Sergey Levine. Entity abstraction in visual model-based reinforcement  
494 learning. In *Conference on Robot Learning*, pages 1439–1456. PMLR, 2020.
- 495 Jane X Wang, Michael King, Nicolas Porcel, Zeb Kurth-Nelson, Tina Zhu, Charlie Deck, Peter Choy,  
496 Mary Cassin, Malcolm Reynolds, Francis Song, et al. Alchemy: A structured task distribution for  
497 meta-reinforcement learning. *arXiv preprint arXiv:2102.02926*, 2021.
- 498 Nicholas Watters, Loic Matthey, Matko Bosnjak, Christopher P Burgess, and Alexander Lerchner.  
499 Cobra: Data-efficient model-based rl through unsupervised object discovery and curiosity-driven  
500 exploration. *arXiv preprint arXiv:1905.09275*, 2019.
- 501 Terry Winograd. Understanding natural language. *Cognitive psychology*, 3(1):1–191, 1972.
- 502 Patrick H Winston. Learning structural descriptions from examples. 1970.
- 503 Kexin Yi, Chuang Gan, Yunzhu Li, Pushmeet Kohli, Jiajun Wu, Antonio Torralba, and Joshua B  
504 Tenenbaum. Clevrer: Collision events for video representation and reasoning. *arXiv preprint*  
505 *arXiv:1910.01442*, 2019.
- 506 Tianhe Yu, Deirdre Quillen, Zhanpeng He, Ryan Julian, Karol Hausman, Chelsea Finn, and Sergey  
507 Levine. Meta-world: A benchmark and evaluation for multi-task and meta reinforcement learning.  
508 *arXiv preprint arXiv:1910.10897*, 2019.
- 509 Xun Zheng, Bryon Aragam, Pradeep K Ravikumar, and Eric P Xing. DAGs with NO TEARS:  
510 Continuous optimization for structure learning. In *Advances in Neural Information Processing*  
511 *Systems*, pages 9472–9483, 2018.

512 **Checklist**

- 513 1. For all authors...
- 514 (a) Do the main claims made in the abstract and introduction accurately reflect the paper's  
515 contributions and scope? [Yes]
- 516 (b) Did you describe the limitations of your work? [Yes]
- 517 (c) Did you discuss any potential negative societal impacts of your work? [Yes]
- 518 (d) Have you read the ethics review guidelines and ensured that your paper conforms to  
519 them? [Yes]
- 520 2. If you are including theoretical results...
- 521 (a) Did you state the full set of assumptions of all theoretical results? [N/A]
- 522 (b) Did you include complete proofs of all theoretical results? [N/A]
- 523 3. If you ran experiments (e.g. for benchmarks)...
- 524 (a) Did you include the code, data, and instructions needed to reproduce the main experi-  
525 mental results (either in the supplemental material or as a URL)? [Yes]
- 526 (b) Did you specify all the training details (e.g., data splits, hyperparameters, how they  
527 were chosen)? [Yes]
- 528 (c) Did you report error bars (e.g., with respect to the random seed after running experi-  
529 ments multiple times)? [Yes]
- 530 (d) Did you include the total amount of compute and the type of resources used (e.g., type  
531 of GPUs, internal cluster, or cloud provider)? [Yes]
- 532 4. If you are using existing assets (e.g., code, data, models) or curating/releasing new assets...
- 533 (a) If your work uses existing assets, did you cite the creators? [Yes]
- 534 (b) Did you mention the license of the assets? [Yes]
- 535 (c) Did you include any new assets either in the supplemental material or as a URL? [Yes]
- 536 (d) Did you discuss whether and how consent was obtained from people whose data you're  
537 using/curating? [N/A] We do not use data from other people.
- 538 (e) Did you discuss whether the data you are using/curating contains personally identifiable  
539 information or offensive content? [N/A] All our data is created using simulation and  
540 does not include any personal information
- 541 5. If you used crowdsourcing or conducted research with human subjects...
- 542 (a) Did you include the full text of instructions given to participants and screenshots, if  
543 applicable? [N/A]
- 544 (b) Did you describe any potential participant risks, with links to Institutional Review  
545 Board (IRB) approvals, if applicable? [N/A]
- 546 (c) Did you include the estimated hourly wage paid to participants and the total amount  
547 spent on participant compensation? [N/A]